Exploring Cryogenic Propellant Behavior in Low-Gravity Environments, Insights from the Saturn AS-203 Vent Experiments and CFD Analysis

Justin Pesich and Daniel Hauser
NASA Glenn Research Center, Fluid and Cryogenic Systems Branch

46th Rocky Mountain AAS GN&C Conference
Feb 2-7, 2024

Motivation

- In the 1960's during NASA's Apollo missions, there was uncertainty on how cryogenic propellants would behave in low gravity environments
- NASA conducted the Saturn AS-203 test flight to investigate the behavior of liquid hydrogen (LH2) while venting the tank below the LH2 saturation pressure[1]
- The experiment aimed to quantify the LH2 fill level fluctuation due to boiling in a state of liquid superheat
- An analytical Boundary Layer Model (BLM) was developed in the 1970's to predict the relative liquid level increase, which estimated the increase to range from 5-15%[2]
- Data from three distinct venting tests revealed minimal changes in the LH2 fill level, corroborating the BLM prediction capability
- There is a need to predict liquid level rise while venting to maintain operational efficiency, particularly at high fill levels

Predicted LH2 Relative Fill Level Increase[2]

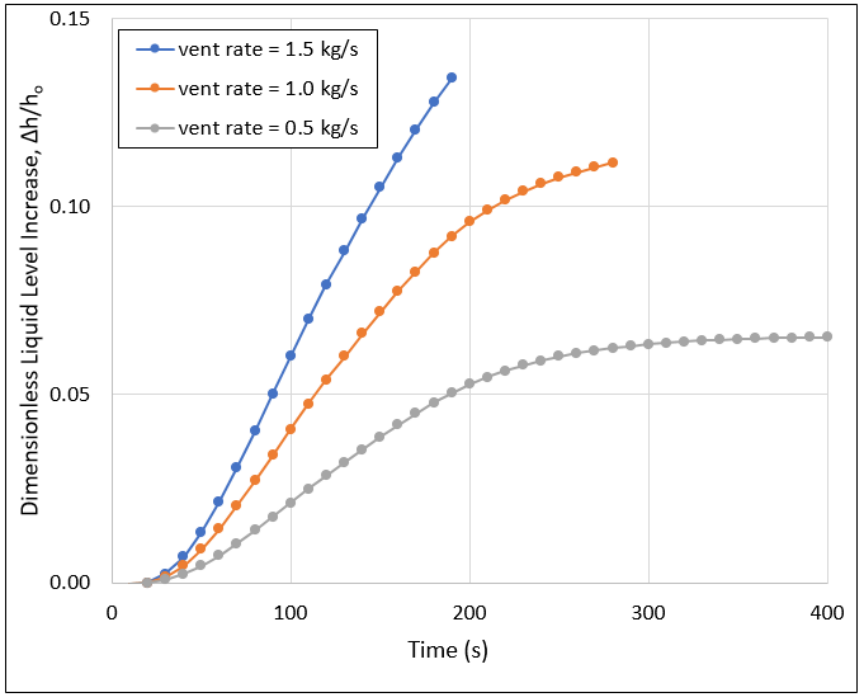

Importance to GN&C:

- Tests were conducted at ~50% fill level, where a 15% increase has a negligible impact
- At a 90% fill level, a 15% increase could result in liquid ejection out vent systems (fuel depots)
- This may introduce asymmetrical force distribution impacting spacecraft control
- In addition, settling thrust while venting must be accounted for while designing GN&C inputs

Saturn AS-203 Test Flight

- Saturn AS-203 flight test was launched July 5, 1966 to a 100 nm circular orbit using the Saturn IB launch vehicle
- Objective was to evaluate the low-gravity performance of the S-IVB upper stage propellant systems (Saturn V's 3rd stage used for TLI)
  - Slosh baffle effectiveness
  - Settling thrusters
  - J-2 engine chilldown systems
  - Fuel tank venting systems
- The current study focuses on the tank depressurization tests, where the fuel tank was vented below the LH2 saturation pressure causing boiling in a superheated liquid
- Vent tests were performed using the non-propulsive vent (NPV) system
- Settling acceleration was applied by both LH2 continuous vent and LOX ullage thrust systems

Saturn AS-203 LH2 Vent System[1]

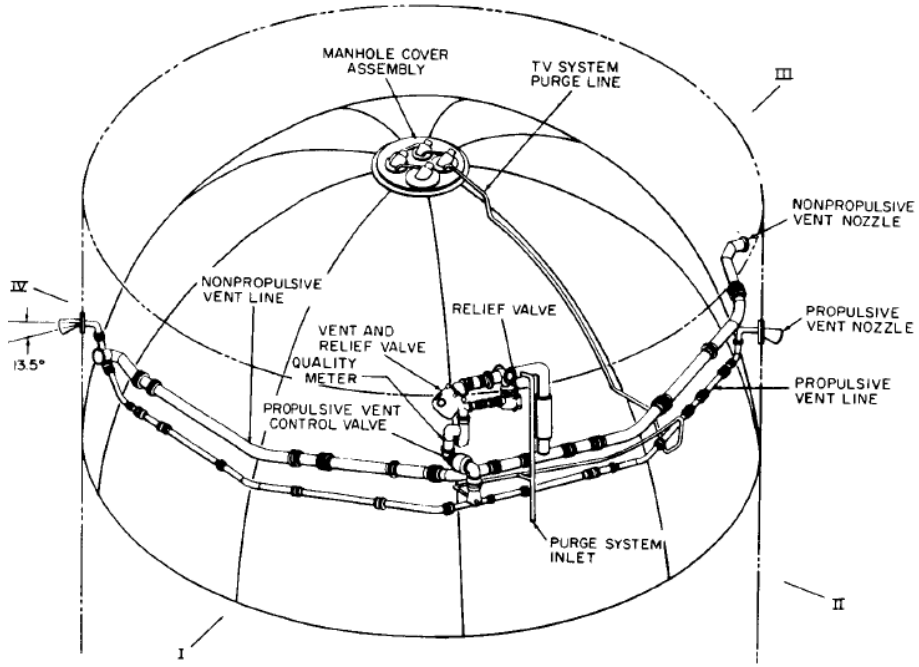

Vent Test Details[1]

Test Detail	First Blowdown	Second Blowdown	Third Blowdown
NPV Open (seconds after liftoff)	14342.2	16723.2	17023.2
NPV Close (seconds after liftoff)	14522.2	16813.2	17113.2
Vent Duration (seconds)	180	90	90
Initial Pressure (psia)	19.5	17.0	14.4
Final Pressure (psia)	13.8	13.0	11.9

CFD modeling case

Saturn AS-203 Depressurization Test: Internal Tank Video

- The Saturn AS-203 flight included temperature and pressure sensors, as well as a camera placed internal to the LH2 tank
- Prior to the first blowdown, video showed liquid in settled state
- Once the NPV was opened, white fog formed obscuring liquid-vapor interface (LVI)
- Once the fog cleared, nearly spherical liquid globules (1-6” in diameter) were observed floating through the ullage
- Wall boiling occurred on internal surfaces and subsequent rapid bubble growth due to liquid superheat possibly “threw” liquid into the ullage

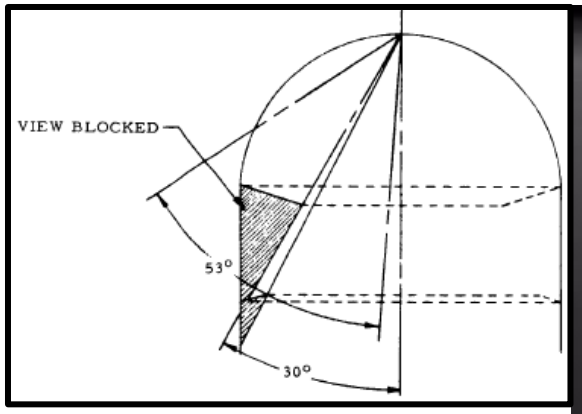

Video shows last 50s of first blowdown

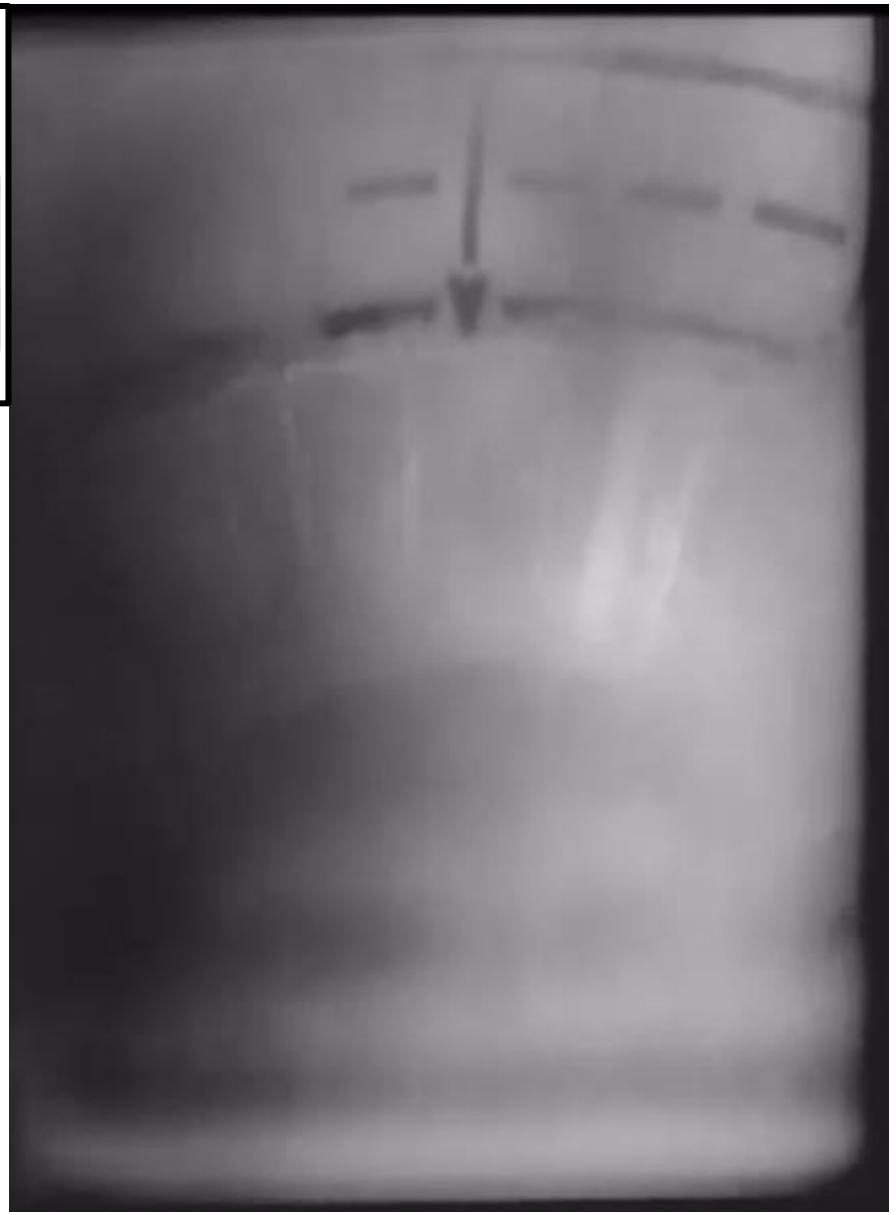

CFD MODEL SETUP

CFD Model Geometry and Mesh

- A 3D 30-degree sector model was used as the input geometry
- The model included slosh baffles but neglected other tank internal structures such as instrumentation rakes and helium bottles
- Two meshes were created to assess mesh-independence
- Fine mesh was refined near the tank wall where bubbles form and bulk LVI
- Solid wall (1 mm) included to model conjugate heat transfer

Saturn-IVB LH2 Tank Dimensions

Dimension	Value
Tank Height (m)	11.320
Tank Diameter (m)	6.630
Vent Pipe Diameter (m)	0.168

3D 30-Degree Sector

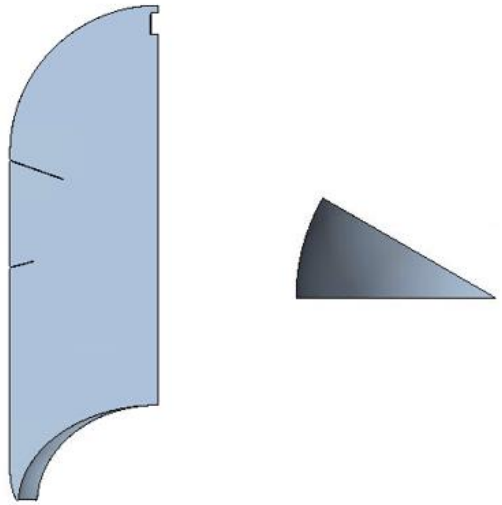

Tank Wall Boundary Identifiers

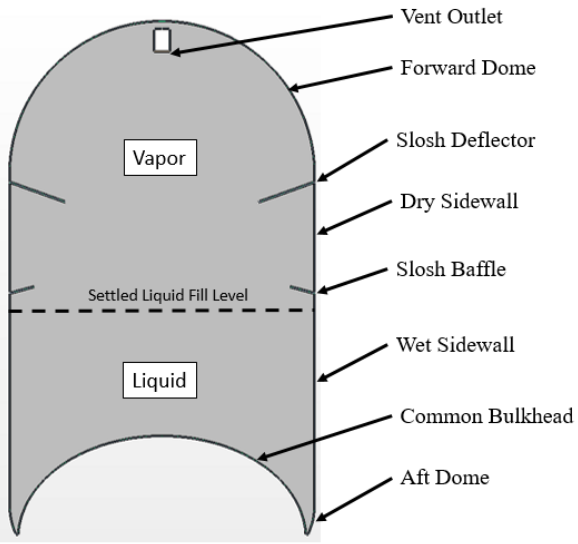

Coarse Mesh

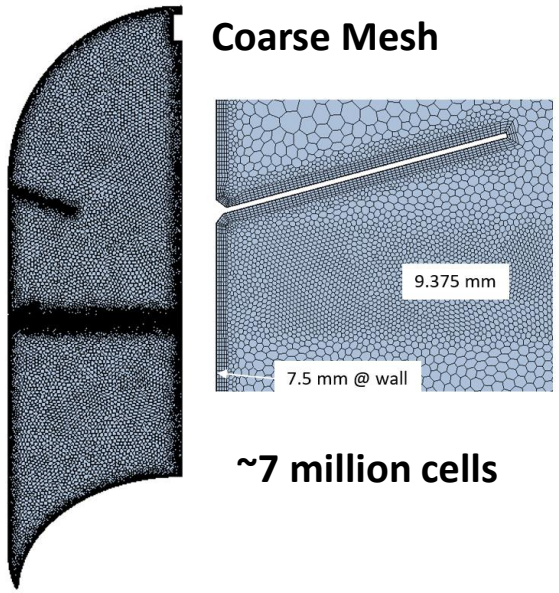

~7 million cells

Fine Mesh

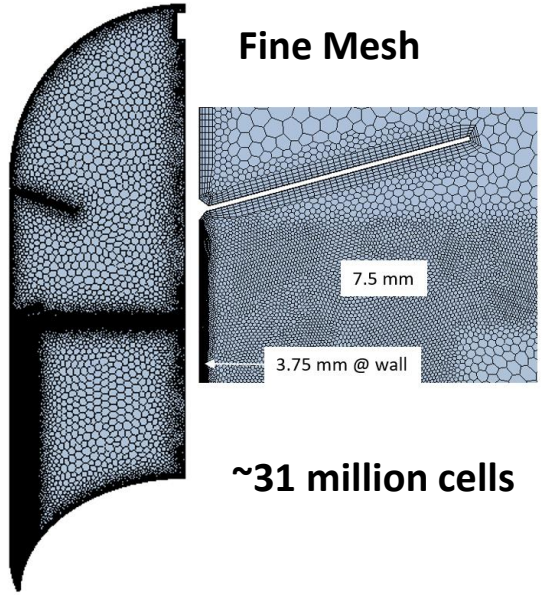

~31 million cells

CFD Initial Conditions and Boundary Conditions

- Initial liquid fill level = 44%
- Initial pressure set to initial pressure measured in experiment (19.5 psi)
- Initial temperature was uniform and set to $T_{sat}(P_{initial})$ = 21.366 K
- Assumed initially quiescent tank ($\mathbf{U}_{initial}$ = [0,0,0])
- Vent mass flow rate prescribed via measured values (~1 kg/s)
- Time-dependent measured heat loads were applied to the outer solid walls for each boundary
- Time-dependent measured settling acceleration was applied as body force (negative values indicate settling aft)

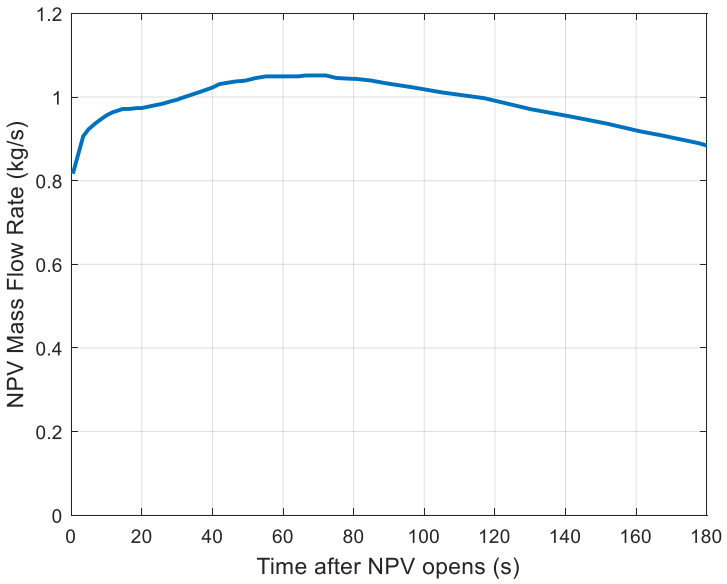

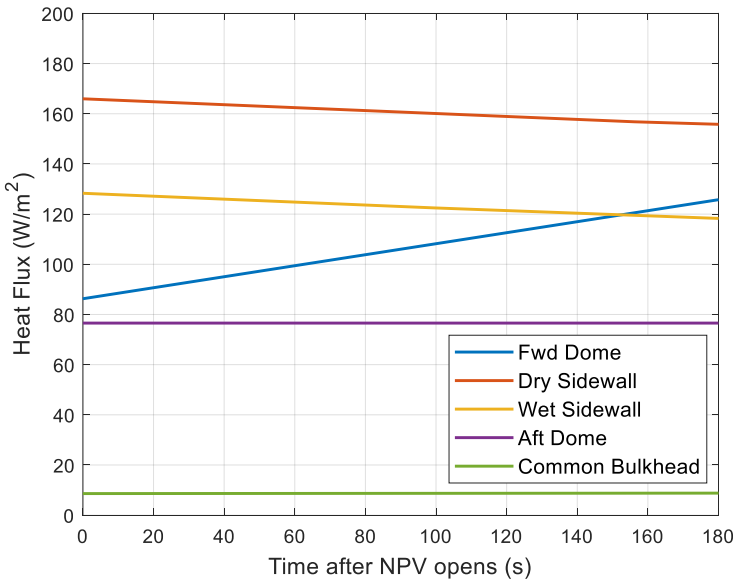

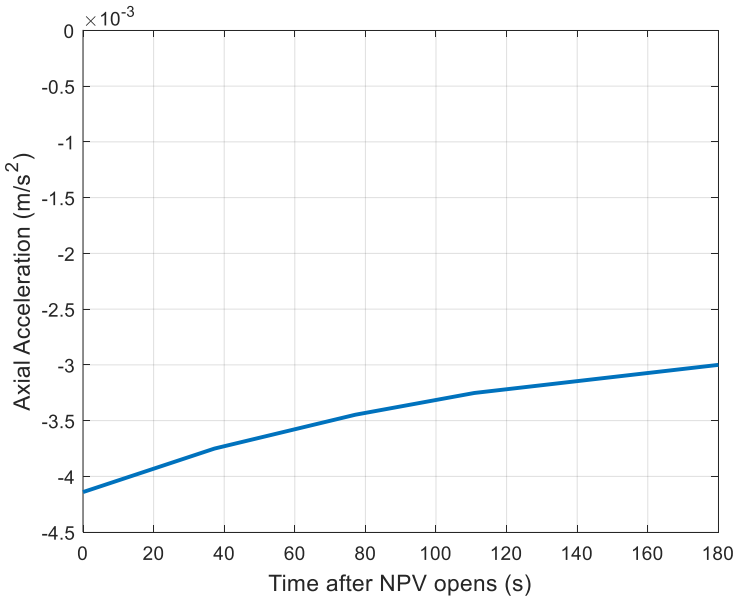

CFD Physics Models

- STAR-CCM+ Volume-of-Fluid (VOF) Multiphase Solver[3]
- Surface Tension Force with 0-degree contact angle[4]
- Constant liquid properties, compressible ideal gas via NIST REFPROP[5] at T_{sat}
- Constant Aluminum 2219 properties[6] at T_{sat}
- Ra_D = 8e11 → turbulent: k-ω Menter SST
- Schrage Equation for user-defined interfacial mass transfer with Accommodation Coefficient, σ
- VOF Transition Boiling Model used for wall boiling
  - Boiling curve is defined by a piecewise function with adjustable coefficients to fit to low-gravity LH2 pool boiling experimental data[7]
  - C_{ew} is the boiling evaporation coefficient

Schrage Equation for Interfacial Mass Transfer

$$\dot{m}_i = \left(\frac{2\sigma}{2-\sigma}\right)\sqrt{\frac{M}{2\pi R T_{cell}}}\left(P_{sat}(T_{cell}) - P_{abs}\right) \quad \left[\frac{kg}{m^2 s}\right]$$

$$\sigma = 0.00001$$

Clausius-Clapeyron Relation

$$P_{sat}(T_{cell}) = P_{ref} exp\left[\frac{L}{R}\left(\frac{1}{T_{ref}} - \frac{1}{T_{cell}}\right)\right]$$

Wall Boiling Mass Transfer

$$\dot{m} = \frac{C_{ew}\dot{q}''_{boiling}}{h_{lat}}$$

C_{ew} is % of boiling heat flux due to evaporation and will depend on fluid, material surface finish, etc.

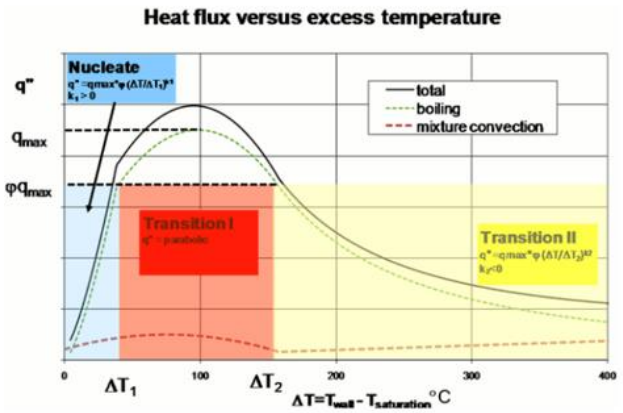

$$q_{boiling}(\Delta T) = q_{max} S\phi\left(\frac{\Delta T}{\Delta T_1}\right)^{K_1} \qquad 0 \le \Delta T \le \Delta T_1$$

$$q_{boiling}(\Delta T) = q_{max} S\left[1 - 4(1-\phi)\left(\frac{\Delta T - \Delta T_{max}}{\Delta T_2 - \Delta T_1}\right)^2\right] \qquad \Delta T_1 \le \Delta T \le \Delta T_2$$

$$q_{boiling}(\Delta T) = q_{max} S\phi\left(\frac{\Delta T}{\Delta T_2}\right)^{-K_2} \qquad \Delta T_2 \le \Delta T$$

Piecewise Boiling Curve Parameters

Parameter	Value
q_{max} (kW/m^2)	47.351
$k1$	2.45
$k2$	20.0
$\Delta T1$ (K)	2.6343
$\Delta T2$ (K)	3.3704
S	1.0
φ	0.75

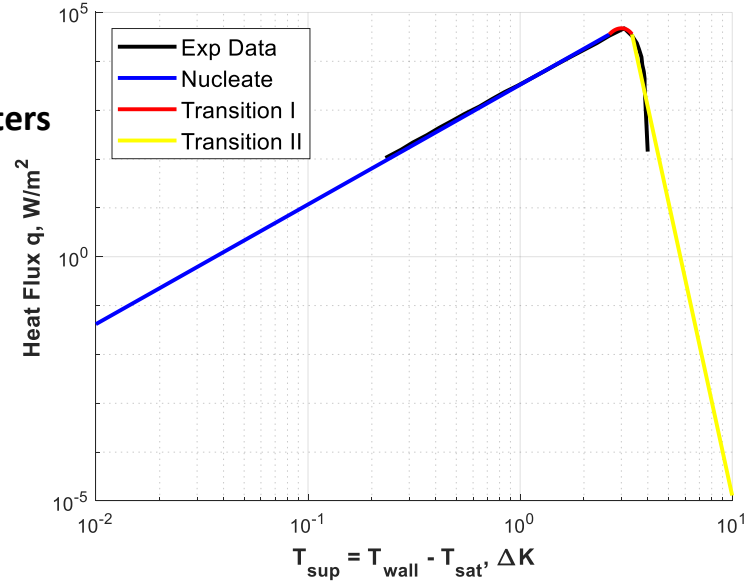

CFD RESULTS

Effect of Boiling Evaporation Coefficient

- CFD pressure and interfacial mass transfer predictions are highly dependent on C_{ew} where higher vapor generation rates will increase pressure
- Slope changes in CFD results indicate onset of nucleate boiling (ONB)
- Test data shows higher pressure than all CFD cases
  - CFD is likely underpredicting amount of vapor generation
  - The model neglected tank internal structures such as instrumentation rakes and helium bottles that provide additional surface area for bubble nucleation
  - Once a nucleation site is activated, bubbles will rapidly grow due to the superheated liquid
- As expected, C_{ew} = 0.2 predicts higher evaporation rate than C_{ew} = 0.1
- C_{ew} = 0.5 case produced much larger bubbles and smeared interfaces, so condensation was occurring inside the bubbles

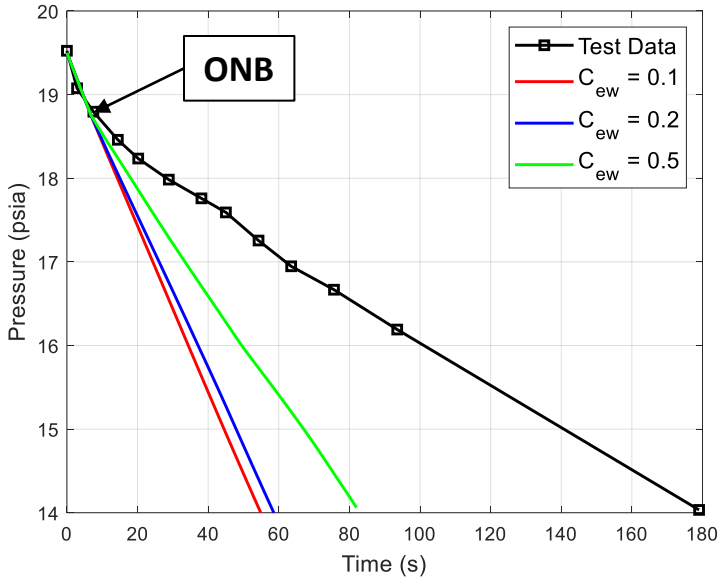

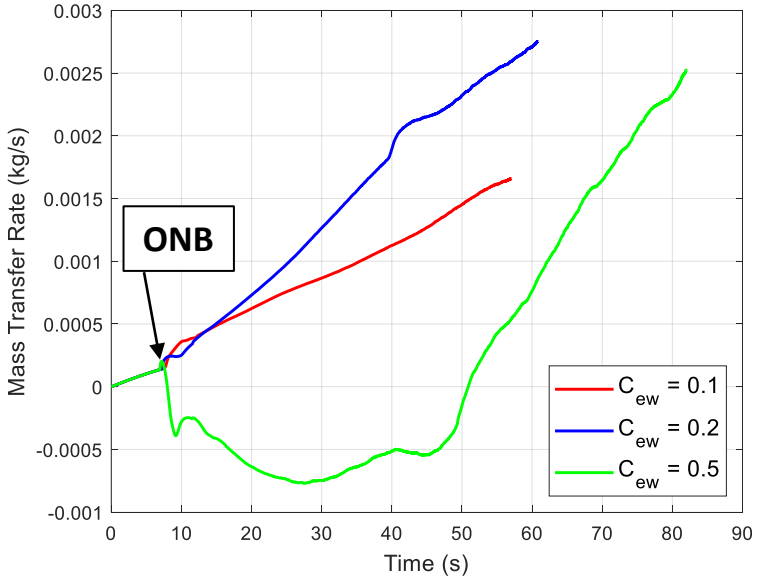

Effect of Boiling Evaporation Coefficient

- Bubble residence time decreased in low gravity due to lower buoyancy force
- Predicted bubble sizes for C_{ew} = 0.5 case appear to be unrealistically large and causes significant liquid level rise

C_{ew} = 0.1

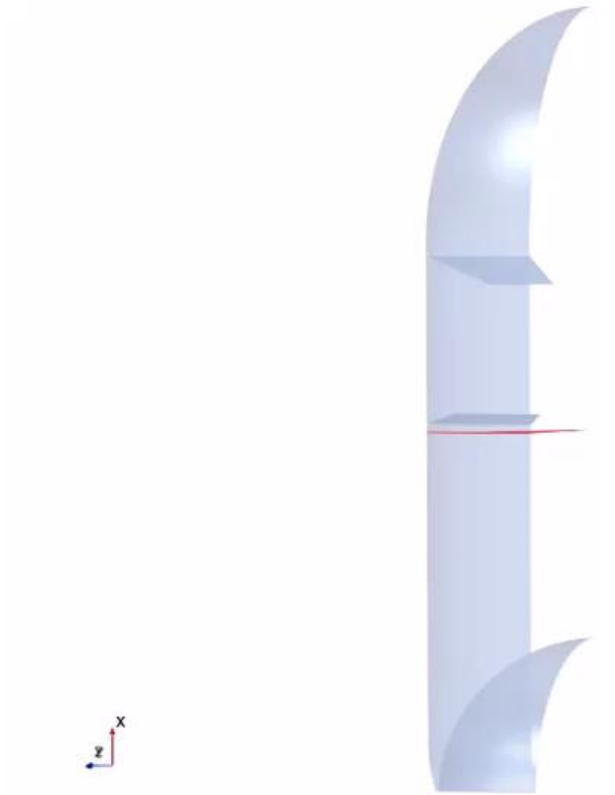

Solution Time 1 (s)

C_{ew} = 0.2

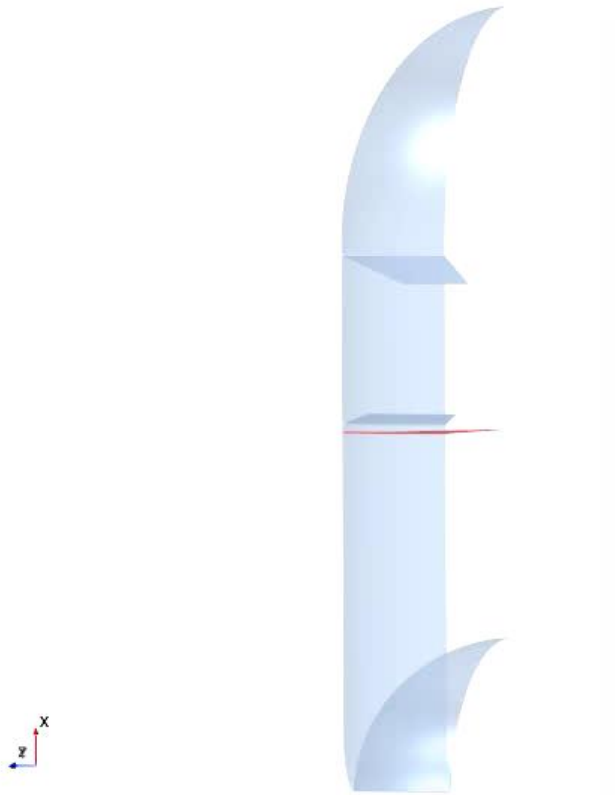

Solution Time 1 (s)

C_{ew} = 0.5

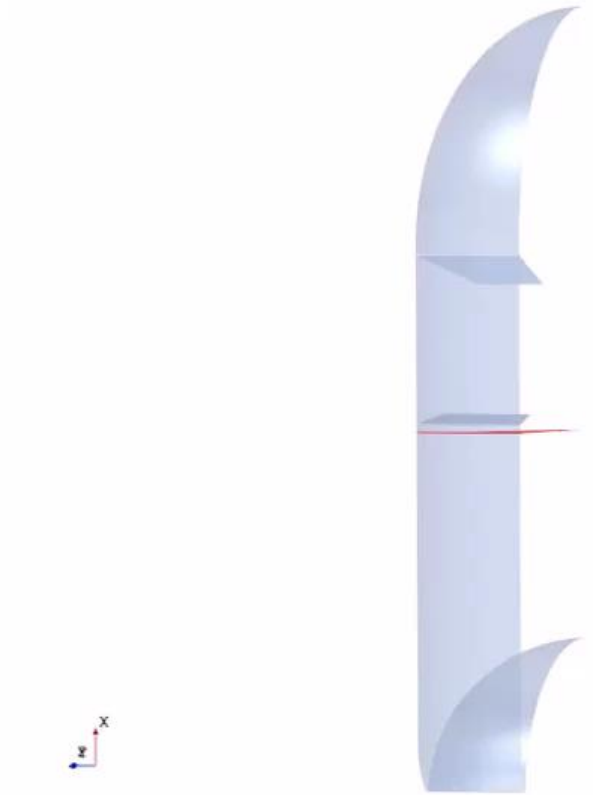

Solution Time 1 (s)

Effect of Mesh Refinement

- The C_{ew} = 0.5 case was run with both the coarse and fine meshes
- The tank pressure is dependent on interfacial mass transfer rates, and interfacial mass transfer rates are dependent on phase distribution
- Higher bubble count and larger bubbles provide more surface area for evaporation to occur
- It was found that the predicted bubble size is directly related to the mesh cell size, and a mesh-independent solution was not attained
- To obtain a mesh-independent solution, the CFD model must be able to resolve bubble nucleation, growth, departure, coalescence, and transport, which is not feasible for most applications (sub-grid models are needed)

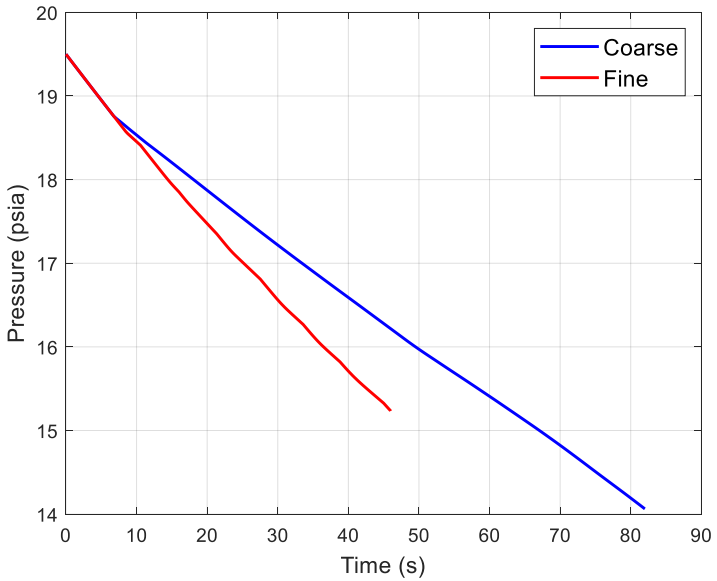

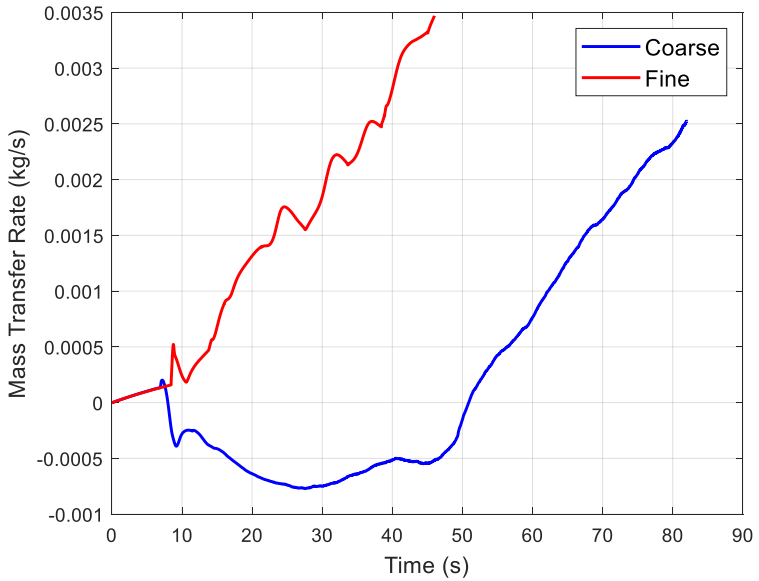

Coarse Mesh **Fine Mesh**

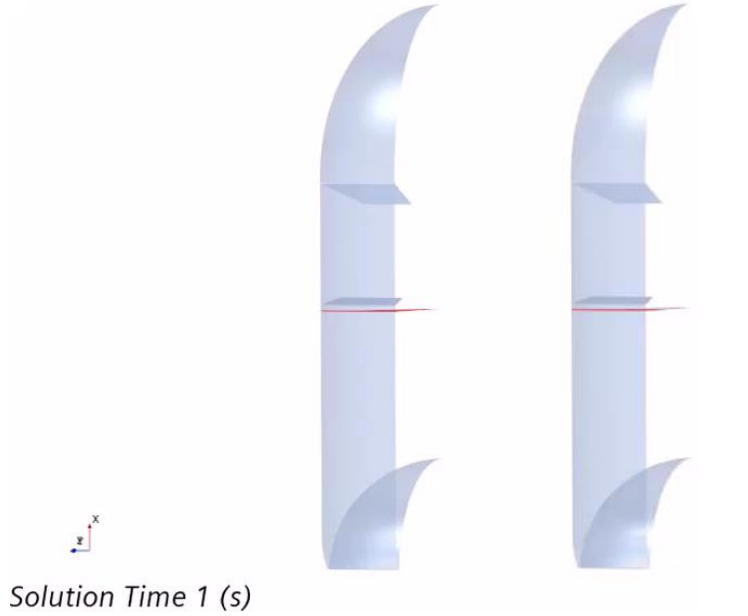

Liquid Level Rise Prediction

- Accurately predicting liquid level rise during venting in low gravity may better inform GN&C spacecraft designers if liquid propellant ejection is a risk, particularly at high fill levels (fuel depots)
- Dimensionless liquid level increase was predicted by both CFD and BLM – both show dependence on boiling evaporation coefficient
- Both predict similar trends and quantities except for the C_{ew} = 0.5 case due to unrealistic bubble sizes
- Up until ONB (~7 seconds), liquid level rise for each CFD case is identical
  - LVI rises due to surface tension and 0-degree contact angle
  - One possible explanation for CFD predicting larger liquid level increases compared to BLM

Relative Liquid Level Rise Predictions for CFD and BLM

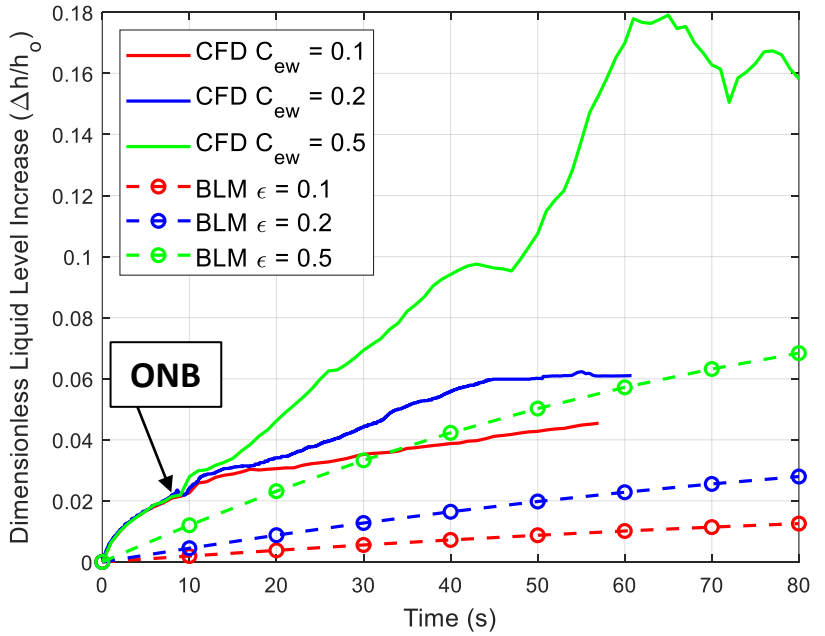

Note: ε for BLM model is essentially equivalent to C_{ew} for CFD

Conclusion

- CFD model predicted minimal liquid level rise in the Saturn-IVB LH2 tank during venting and is in agreement with the analytical Boundary Layer Model developed in the 1970's
- Both models demonstrate a strong correlation to the boiling evaporation coefficient
- Modeling challenges such as mesh-dependence and resolving bubble interfaces highlight the need for a sub-grid model to accurately resolve bubble nucleation, growth, departure, and transport
- Implications of liquid level rise during venting in low gravity, especially at higher fill levels, are particularly relevant to GN&C designers for spacecraft, in addition to settling thrust maneuvers
- Although CFD presents a significant advancement in technology, there is a continuous need to refine these techniques to overcome numerical issues and improve our understanding and predictions of cryogenic fluid management in space environments

Acknowledgments

This work was funded by the Cryogenic Fluid Management Modeling Portfolio and Cryogenic Fluid Management Portfolio Project under the Space Technology Mission Directorate at NASA. The authors recognize Bruce Ciccotosto for performing 2D and 3D simulations of the Saturn AS-203 vent test and for extracting all the experimental data from the reports. The authors also recognize Matthew Moran for his work and insight on the analytical venting model.

References

1. Chrysler Corporation Space Division, “Evaluation of AS-203 Low Gravity Orbital Experiment,” NASA-CR-94045, 1967.
2. Bradshaw, R. D., “Evaluation and Application of Data from Low-Gravity Orbital Experiment, Phase I Final Report,” NASA-CR-109847, 1970.
3. Siemens Simcenter STAR-CCM+, Ver. 14.02.010-R8 (2019.1), Plano, TX,2019.
4. Brackbill J. U., Kothe, D. B., Zemach, C., “A continuum method for modeling surface tension,” J. Comp. Phys. Vol. 100, 1992, pp. 335–354.
5. NIST REFPROP, Ver. 9.1, Boulder, CO, 2013.
6. Marquardt, E. D., Le, J. P., Radebaugh, R., “Cryogenic Material Properties Database,” 11th International Cryocooler Con-ference, Keystone, CO, 2000.
7. Lei W., Kang Z., Fushou X., Yuan M., Yanzhong L., “Prediction of pool boiling heat transfer for hydrogen in micro-gravity,” International Journal of Heat and Mass Transfer. Vol. 94, 2016, pp. 465-473.

YouTube link to fuel tank camera video for Saturn AS-203 test flight:
https://www.youtube.com/watch?v=mJzT2bBGVfo&t=990s

Notation

BACKUP

Importance to GN&C

4. Vent System Thrust Unbalance

During the three blowdown sequences, it was observed that the auxiliary propulsion system engines were excessively active in providing control about the yaw axis, indicating a significant unbalanced force between the two sides of the non-propulsive vent system. During the first blowdown (180 second duration) the number two yaw engine in Module I (I_2) fired 29 times and the number two engine in Module III (III_2) fired 22 times. During the second blowdown, I_2 and III_2 fired 16 and 11 times, respectively, and during the third blowdown they fired 7 and 4 times, respectively. This firing frequency represents the highest APS activity during the entire flight, except at orbital insertion. Other than during the blowdown sequences, these particular engines were the least active of the APS system. The non-propulsive vent system ΔP measurement (D215) fluctuated rapidly and indicated a significant differential between the vent system branches during all three tests substantiating the fact that venting from the NPV system had produced an unbalanced force on the vehicle. The pressure differential during the blowdowns varied from zero to -0.40, -0.36, and -0.26 psi during the first, second, and third tests, respectively. Figure VI-5 illustrates the ΔP fluctuation during the first blowdown. The maximum unbalanced thrust resulting from the unbalanced pressure during the first blowdown is calculated to be about 3.85 lb_f.

Text reproduced from Reference 1

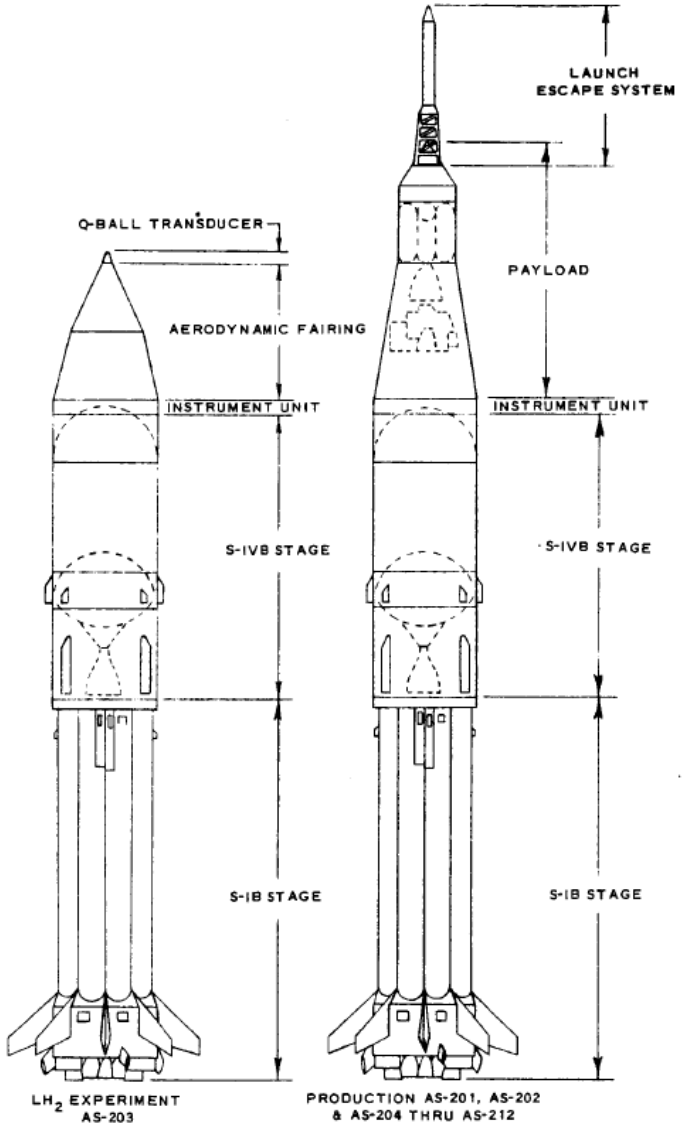

Picture reproduced from Reference 1

LH2 Vent System

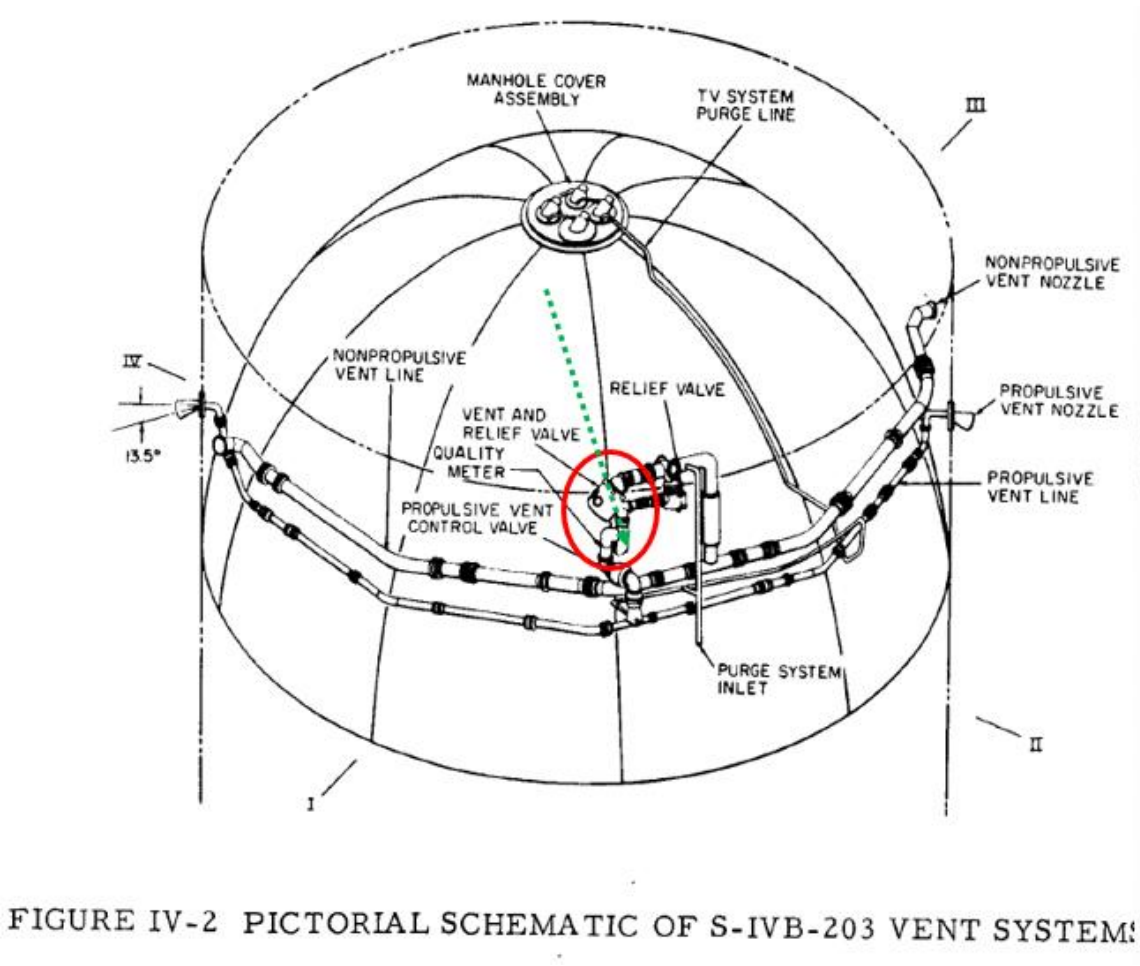

FIGURE IV-2 PICTORIAL SCHEMATIC OF S-IVB-203 VENT SYSTEM

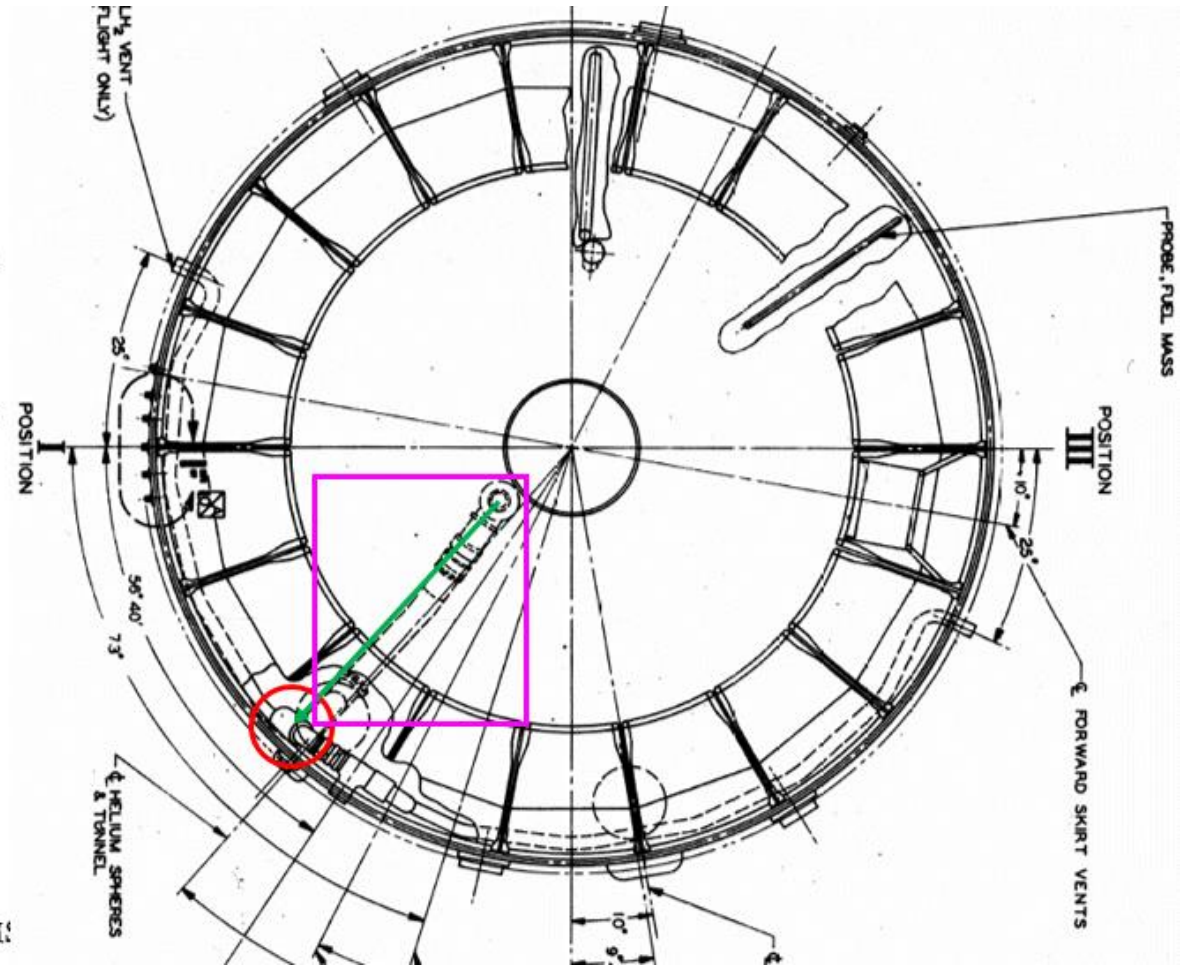

Picture reproduced from Reference 1